Dissociation of multicharged CO molecular ions produced in collisions with 97-MeV Ar^{14+}: Dissociation fractions and branching ratios

K. Wohrer,* G. Sampoll, R. L. Watson, M. Chabot,† O. Heber,‡ and V. Horvat§
Cyclotron Institute, Texas A&M University, College Station, Texas 77843
and Department of Chemistry, Texas A&M University, College Station Texas 77843
(Received 1 April 1992)

Data on the production and dissociation of CO^{Q+} molecular ions (where $Q=1$ through 7) obtained by ion-ion coincidence time-of-flight measurements were analyzed to determine production yields, dissociation fractions, and branching ratios. A detailed comparison of the dissociation fractions for CO^+ and CO^{2+} for several collision systems in the same perturbative regime revealed them to be quite similar, whereas the dissociation fraction for CO^+ produced by valence-electron photoionization is a factor of 1.8 to 3.6 larger. The results for $Q \geq 2$ indicated a preference for dissociation channels leading to symmetric or nearly symmetric charge division. An enhancement of the total ionization yields for $Q > 4$ was observed, and it suggests that electron transfer followed by *LMM* Auger decay plays an important role in determining the final charges of the dissociation products.

PACS number(s): 34.50.−s, 35.80.+s, 34.90.+q

I. INTRODUCTION

In a recent investigation conducted in this laboratory, coincidence time-of-flight (TOF) spectroscopy was used to identify the dissociation products from transient molecular ions of CO^{Q+} (where $Q=2-7$) produced in single collisions of 97-MeV Ar^{14+} ions with neutral CO molecules [1]. A two-parameter data-acquisition system was employed to record both the TOF of the first dissociation product ion to pass through the spectrometer and the difference in the flight times of the first ion and its partner for each detected binary dissociation event. Subsequent off-line sorting of the data provided well-resolved time-difference distributions for each of the prominent charge division pathways. These time-difference distributions were transformed into total-kinetic-energy distributions, which, in turn, provided information concerning the average excitation energies of the parent molecular ions.

In this paper, the dissociation product yields obtained in the above experiment are used to determine dissociation fractions for CO^+ and CO^{2+}, and branching ratios for the different charge division pathways observed in the dissociation of CO^{3+} to CO^{7+}. The present results for CO^+ and CO^{2+} are compared with those obtained by Hitchcock *et al.* [2] using valence-electron photoionization, and by Shah and Gilbody [3] using 16-keV H^+ and 260-keV He^{2+} ion impact. The projectiles in this latter study were chosen for comparison because they reside in the same perturbative regime as 97-MeV Ar^{14+}. The branching ratios for the dissociation of multicharged CO molecular ions and the total ionization yields are presented and examined for revelations concerning the major factors that govern the relative probabilities of the various charge-division pathways.

II. EXPERIMENTAL METHODS

A detailed description of the experimental methods employed to make the measurements is contained in Ref. [1]. Only a brief summary is presented here. A beam of 97-MeV Ar^{14+} ions from the Texas A&M K500 superconducting cyclotron was focused onto the entrance aperture of a differentially pumped gas cell containing 1×10^{-3} Torr of CO. After passing through the cell, the beam impinged on a microchannel plate (MCP) detector assembly and generated stop signals for the time-of-flight measurements. Ions produced in the gas cell as a result of the dissociation of CO molecules ionized in collisions with Ar ions were accelerated out of the cell by a transverse electric field into a flight tube. Those ions that traveled through the flight tube were detected by another MCP assembly, which provided start signals for the TOF measurements. Two parameters—the flight time of the first dissociation-product ion to pass through the spectrometer and the difference in flight times of the first ion and its partner—were measured and recorded on magnetic tape event by event. A noncoincidence (singles) TOF spectrum of all ions passing through the TOF spectrometer, without the requirement that both ions of each binary dissociation event be detected, was recorded simultaneously using a separate multichannel pulse-height analyzer.

III. DATA ANALYSIS

The data obtained for CO are shown in the form of a two-dimensional plot of first-ion TOF versus ion-pair time difference in Fig. 1(a). Projection of these data onto the TOF axis yields the total first-ion TOF spectrum [Fig. 1(b)], while projection onto the time-difference axis yields the total ion-pair time-difference spectrum [Fig. 1(c)]. By placing windows around the various TOF peaks in the total first-ion TOF spectrum and projecting only events within these windows onto the time-difference axis, separate time-difference spectra were obtained for each ion pair. The sorted time-difference spectra obtained for C^+ through C^{4+} and O^+ through O^{3+} windows are shown in Ref. [1].

Total detection yields $[N(I)]$ of single ions were deter-

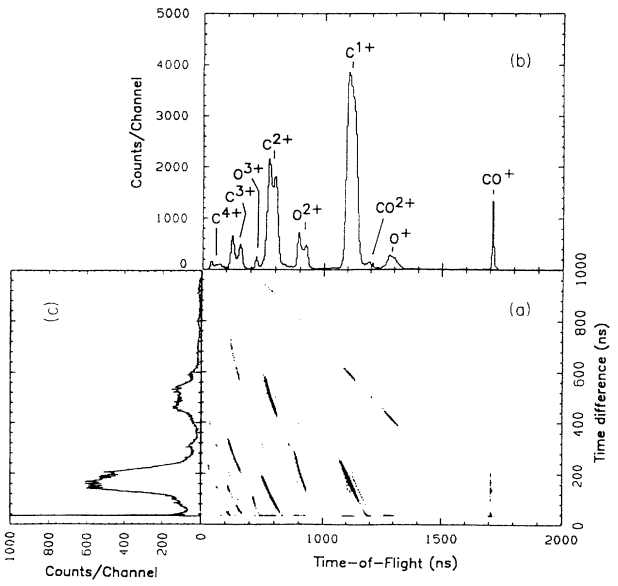

FIG. 1. A two-dimensional display of the data for the dissociation of multicharged CO molecular ions. The portion labeled (a) shows the first-ion time of flight (TOF) vs the ion-pair flight time difference. Projection of this data onto the TOF axis yields the first-ion (coincidence) TOF spectrum (b), while projection onto the time-difference axis yields the total ion-pair time-difference spectrum (c).

mined by integrating the corresponding peaks in the singles TOF spectrum after subtraction of a linear background. In cases where two or more peaks overlapped, a Gaussian peak fitting program was used to calculate the individual yields. The single-ion production yields $[Y(I)]$ were then obtained using the relationship

$$Y(I)=N(I)(T_{1s}T_g\epsilon_d)^{-1}\ , \tag{1}$$

where T_{1s} is the single-ion transmission probability through the TOF spectrometer, T_g is the product of the transmission probabilities through the set of grids at the entrance and at the exit of the flight tube (0.77), and ϵ_d is the detection efficiency of the MCP ion detector at the end of the flight tube.

Total detection yields of ion pairs $[N(I_1+I_2)]$ were determined by integrating the corresponding ion-pair time-difference distributions. These yields were corrected for background and for contributions due to double collisions by the projectile while passing through the gas cell. Well-separated double-collision peaks were observed in the sorted time-difference spectra for the ion pairs $(CO^{2+}+CO^+)$, (O^++CO^+), $(CO^{2+}+O^+)$, (C^++CO^+), and $(C^{2+}+C^+)$. Since the dectection yield of a double-collision peak $N_d(I_1+I_2)$ is proportional to the product of the detection probabilities of the individual ions, it may be expressed in terms of the yield of any other double-collision peak having an ion in common:

$$N_d(I_1+I_2)=N_d(I_1+I_3)[N(I_2)/N(I_3)]\ . \tag{2}$$

The above relationship was used along with the single-ion detection yields to calculate the number of counts due to double collisions under the ion-pair time-difference distributions of interest. Corrections for double-collision contributions were typically 4% or less. The ion-pair production yields were then obtained using the relationship

$$Y(I_1+I_2)=N(I_1+I_2)[T_{12s}T_g^2\epsilon_1\epsilon_2]^{-1}\ , \tag{3}$$

where T_{12s} is the ion-pair transmission probability through the spectrometer and the other quantities are as defined above.

In the following analysis, the total dissociation yield for a specific parent molecular ion $Y_D(M)$ is defined as the sum of the production yields of all possible dissociation product pairs formed within a time interval determined by the flight time of the molecular ion to the entrance of the flight tube. The time restriction is imposed by the fact that molecular ions that dissociated after entering the flight tube were still detected as molecular ions, since, at that point, they had been fully accelerated. In particular, the dissociation yields for CO^+ and CO^{2+} are

$$\begin{aligned} Y_D(CO^+)&=Y(C^++O)+Y(C+O^+)\ , \\ Y_D(CO^{2+})&=Y(C^{2+}+O)+Y(C^++O^+) \\ &\quad +Y(C+O^{2+})\ , \end{aligned} \tag{4}$$

and the pertinent time intervals are 0.30 and 0.21 μs, respectively. Then the fractions α of molecular ions that dissociate within these time intervals are given by

$$\begin{aligned} \alpha(CO^+)&=\frac{Y_D(CO^+)}{Y_D(CO^+)+Y(CO^+)}\ , \\ \alpha(CO^{2+})&=\frac{Y_D(CO^{2+})}{Y_D(CO^{2+})+Y(CO^{2+})}\ . \end{aligned} \tag{5}$$

Since CO^+ has a stable ground state and the ground state of CO^{2+} is known to have a lifetime greater than 15 μs [4], the dissociation fractions determined by the short acceleration time scale of this experiment provide measures of the total excitation probabilities to short-lived autodissociative states.

Since only ions were detected in the present experiments, the production yields of dissociation product pairs in cases where one of the products was neutral had to be determined using the single-ion production yield of the charged partner and the ion-pair production yields for all ion pairs involving that partner. For example, the production yields of (C^++O) and $(C+O^+)$ pairs from the dissociation of CO^+ were obtained using the following expressions:

$$\begin{aligned} Y(C^++O)&=Y(C^+)-\sum_{n\neq 0}Y(C^++O^{n+})\ , \\ Y(C+O^+)&=Y(O^+)-\sum_{n\neq 0}Y(C^{n+}+O^+)\ . \end{aligned} \tag{6}$$

A computer program was developed to calculate the probabilities for single-ion and ion-pair transmission through the spectrometer. It incorporated a Monte Carlo procedure to simulate statistical distributions of the

starting coordinates and velocity components of the ions. In calculating the ion-pair transmission probabilities, the trajectories of both dissociation product ions were followed for each simulated event until either both ions reached the MCP detector or until one of them collided with the gas-cell wall, the flight-tube wall, or the collimator separating the gas cell from the flight tube. The program also took into account the possibility that an ion might undergo a charge-exchange collision with a neutral CO molecule on the way to the flight tube. The transmission probability was obtained by dividing the number of "successful" events, for which both ions made it all the way to the MCP, by the number of attempted events. Details of the calculations are given in Ref. [1]. As shown in Fig. 2 for the ion pair $(C^+ + O^+)$, the ion-pair transmission probabilities were fairly sensitive to the initial kinetic energies of the ions. The ion-pair transmission probabilities employed in the present data analysis were calculated using the experimental kinetic-energy distributions determined in the work described in Ref. [1] and are expected to be accurate at the level of $\pm 10\%$.

The detection efficiency of an MCP detector for keV ions is extremely difficult to determine experimentally and only a few studies of this quantity have been reported in the literature. Since the ions were accelerated through a total potential of 2599 V, the energy range of interest here extends from 2.60 keV for the $q=1+$ ions to 10.39-keV for the $q=4+$ ions. According to data obtained by various investigators [5–8], MCP efficiencies may range from 0.3 to 0.7 at 2 keV and from 0.5 to 0.8 at 10 keV. In the present analysis, the efficiency has been assumed to be equal to the open (channel) area fraction of the MCP, which was 0.55. The validity of this assumption has been verified experimentally for He^+ ions in the energy range of 1–10 keV by Tobita *et al.* [9]. However, in order to estimate the error introduced into the results by the large uncertainty in the MCP detection efficiency, the data analysis was perfomred also with both the high and the low value of the range for each ion energy. Because a certain amount of cancellation occurs in the ratios that define the dissociation fractions [see Eq. (5)], the errors in the results are substantially less than those in the MCP

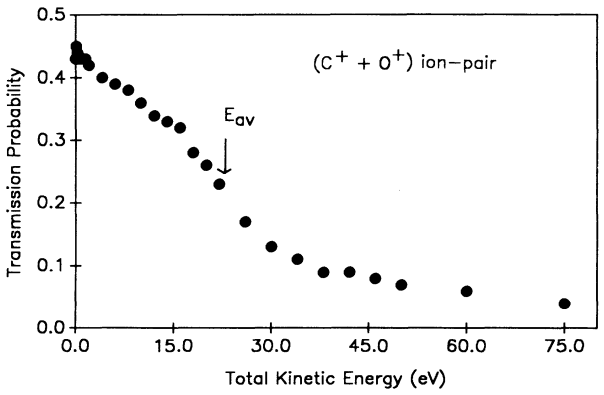

FIG. 2. The calculated spectrometer transmission probability for the ion pair $(C^+ + O^+)$ as a function of the total kinetic energy. The average total kinetic energy of the ion pair is indicated by the arrow.

efficiencies, expecially for $\alpha(CO^{2+})$. Moreover, it was found that the production yield for the ion pair $(C+O^{2+})$ became negative when efficiency values of less than 0.45 were used. The requirement that this yield be ≥ 0 further reduced the error associated with the MCP efficiencies.

As mentioned above, the spectrometer transmission probability calculations included events in which the ion captured an electron in a collision with a neutral CO molecule on its way to the flight tube. This was necessitated by the observation of a tail containing 22% of the total counts on the longer-time side of the TOF peak for the CO^+ ions. A study of the shape of this peak as a function of CO pressure revealed that approximately 13% of the counts in the tail were attributable to electron-capture events. Peak simulation calculations established that a capture probability of $(5\pm 3)\%$ was consistent with the fraction of the CO^+ tail attributed to capture. A similar analysis of the O^{2+} peak yielded a capture probability in the same range. This value was used in all of the spectrometer transmission probability calculations. The uncertainty associated with the capture probability translated into a 2% uncertainty in the calculated transmission probability, on average. The effect of capture was to increase the transmission probability for ions having little or no initial kinetic energy and decrease the transmission probability for energetic ions. As a result of this, the tails observed in the TOF peaks for the dissociation-product ions were substantially smaller than those observed for the very-low-energy CO^+ and CO^{2+} molecular ions.

IV. RESULTS AND DISCUSSION

The dissociation fractions and ion-pair production yields for CO^+ and CO^{2+} are listed in Table I. Since direct Coulomb ionization of valence electrons is expected to be the dominant ion-production mechanism for collisions of 2.4-MeV/amu Ar^{14+} ions [10], these results are compared with those obtained by Hitchcock *et al.* [2] for valence-electron photoionization by 280-eV synchrotron radiation, and by Shah and Gilbody [3] for direct valence-electron ionization by 16-keV/amu H^+ and 65-keV/amu He^{2+} ions. The ion-molecule systems all have nearly the same values of the parameter

$$K=(Z_p/Z_t)(v_e/v_p)\,, \tag{7}$$

where Z_p, Z_t, v_e, and v_p are, respectively, the projectile and target atomic numbers, and the valence electron and projectile velocities. The quantity K is a measure of the strength of the perturbation presented to the valence electrons during a collision [11]. It is apparent that all three ion-molecule systems display fairly similar characteristics, with the $(C^+ + O)$ dissociation channel being considerably preferred over the $(C+O^+)$ dissociation channel. In the case of CO^{2+}, the symmetric charge division pathway leading to $(C^+ + O^+)$ is greatly preferred over the asymmetric charge division channels, and it is evident also that the branching ratio for producing doubly ionized C ions is considerably enchanced relative to the branching ratio for producing doubly ionized O

TABLE I. Dissociation fractions and production yield ratios for CO^+ and CO^{2+}.

	Present work	Shah and Gilbody [3]		Hitchcock *et al.* [2]
Ratio	97-MeV Ar^{14+}	16-keV H^{1+}	261-keV He^{2+}	280-eV photons
$\alpha(CO^+)$	0.33±0.08	0.44±0.04	0.22±0.04	0.8
$Y(C^+ + O)/Y(CO^+)$	0.31±0.08	0.58±0.08	0.23±0.03	1.6
$Y(C + O^+)/Y(CO^+)$	0.21±0.11	0.19±0.03	0.06±0.01	1.6
$Y(C^+ + O)/Y(C + O^+)$	1.8±0.7	3.1±0.8	3.8±1.0	1.0
$\alpha(CO^{2+})$	0.95±0.02			0.9
$Y(C^+ + O^+)/Y(CO^{2+})$	14.5±4.3	12.1±1.8[a]	14.6±2.9[a]	6.5
$Y(C^{2+} + O)/Y(CO^{2+})$	3.2±2.2			3.0
$Y(C + O^{2+})/Y(CO^{2+})$	0.7±0.7			1.0
$Y(C^{2+} + O)/Y(C + O^{2+})$	4.6±1.8			3.0

[a]These values are for transfer ionization.

ions. This is understandable on the basis of the atomic ionization energies, since 48.8 eV is required to remove two electrons from oxygen while only 35.6 eV is required to remove two electrons from carbon. The minimum excitation energy required by the $(C^+ + O^+)$ dissociation branch is nearly the same as that for the $(C^{2+} + O)$ branch because, in addition to the ionization energies of C and O (24.9 eV), the Coulomb repulsion energy (≈ 12.8 eV) must also be supplied.

The photoionization results of Hitchcock *et al.* [2] for single ionization of CO are quite different than those obtained by ion-impact ionization. In particular, the dissociation fraction for CO^+ is much larger, implying that valence-electron photoionization at 280 eV is considerably more effective in populating short-lived autodissociative states than ion-impact ionization. On the other hand, the dissociation fractions for CO^{2+} are essentially the same for both ionization mechanisms.

Because of the large contribution to the singles TOF spectrum of C^+ ions from the $(C^+ + O)$ dissociation channel ($\approx 60\%$), it was possible to estimate the $(C^+ + O)$ total kinetic-energy distribution. This was accomplished by performing simulation calculations of the shapes and intensities of the TOF peaks produced by the other contributing channels, $(C^+ + O^+)$ and $(C^+ + O^{2+})$. After subtracting these calculated contributions, the residual TOF peak was analyzed to obtain the total kinetic-energy distribution. The results gave a broad structure shaped like a Gaussian with its left side truncated at 0 eV and the tail of its right side extending up to 25 eV. The most probable and the average energies of this distribution were approximately 3 and 8 eV, respectively.

The relative production yields of ion pairs produced in the dissociation of CO^{Q+} with $Q=2-7$ are listed in Table II. In general, the same preference for charge-symmetric or nearly-charge-symmetric dissociation channels as was observed for CO^{2+} is evident in these data. It is to be expected that, in most collisions, the ionization will be localized along the projectile trajectory. This means that most of the electron vacancies produced in a collision initially will be localized about either the C or the O atom and hence considerable rearrangement must occur during the initial stages of the dissociation process.

To aid in the following discussion, the estimated minimum excitation energies required for all of the possible charge division channels are displayed in Fig. 3. These excitation energies were calculated with the formula

$$E_{\min}(q_1,q_2) \simeq D_0 + \sum_{i=1}^{q_1} B_i(\mathrm{C}) + \sum_{j=1}^{q_2} B_j(\mathrm{O}) + \mathrm{CE}\ , \qquad (8)$$

where q_1 and q_2 are, respectively, the charges of the carbon- and oxygen-ion dissociation products, D_0 is the dissociation energy of the neutral molecule (11.1 eV), $B_i(\mathrm{C})$ is the ith ionization energy of the carbon atom, $B_j(\mathrm{O})$ is the jth ionization energy of the oxygen atom, and CE is the point-charge Coulomb potential energy $q_1 q_2 / R$, where R is the neutral molecule bond length (1.128 Å). Figure 3 shows that, for a given total charge Q, the lowering of the total ionization energy that results from equalizing the carbon- and oxygen-ion charges is, for the most part, canceled by the attendant increase in the Coulomb energy. The net result is that there is not much of a change in the minimum excitation energy required for any charge division pair (having the same Q) unless formation of the pair involves the removal of a K-shell electron, in which case the excitation energy rises abruptly (see the curves for $Q=5$, 6, and 7). Nevertheless, for $Q=3$ the minimum excitation energy required for the $(C^{2+} + O^+)$ channel is approximately 11 eV lower than that for the $(C^+ + O^{2+})$ channel and the data in

TABLE II. Relative production yields of ion pairs from the dissociation of CO^{Q+}.

Q	$(I_1 + I_2)$	$Y(I_1 + I_2)/Y(C^+ + O^+)$
2	$(C^+ + O^+)$	1
3	$(C^{2+} + O^+)$	0.45±0.04
	$(C^+ + O^{2+})$	0.20±0.02
4	$(C^{3+} + O^+)$	0.059±0.006
	$(C^{2+} + O^{2+})$	0.26±0.03
5	$(C^{3+} + O^{2+})$	0.13±0.01
	$(C^{2+} + O^{3+})$	0.13±0.03
6	$(C^{3+} + O^{3+})$	0.29±0.04
	$(C^{4+} + O^{2+})$	0.024±0.006
7	$(C^{4+} + O^{3+})$	0.04±0.04

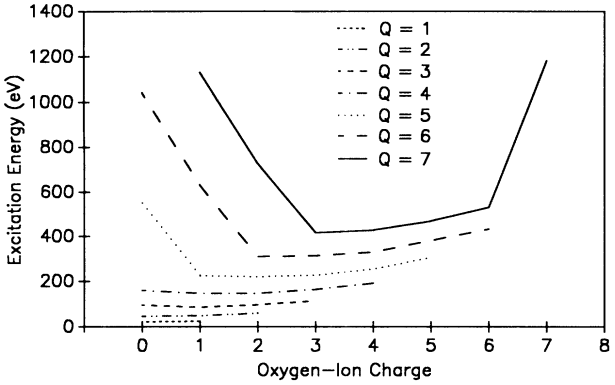

FIG. 3. The estimated minimum excitation energy required to produce ion pairs ($C^{q_1}+O^{q_2}$) vs the charge (q_2) of the oxygen ion, where $Q=q_1+q_2$.

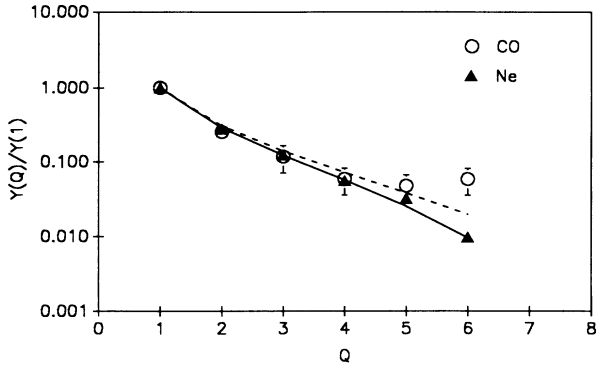

FIG. 4. The ratio of the total ionization yield for charge Q, $Y(Q)$, to the total ionization yield for $Q=1$. The solid and dashed lines show the results of independent-electron-approximation calculations for Ne and CO, respectively, as explained in the text.

Table II clearly indicate that the former channel is favored. On the other hand, for $Q=4$, the data in Table II indicate that there is a very strong preference for the symmetric ($C^{2+}+O^{2+}$) channel over the asymmetric ($C^{3+}+O^{+}$) channel, while the estimated minimum excitation energies for these two dissociation channels are both the same. Moreover, for $Q=5$, the estimated minimum excitation energies required for the three channels ($C^{4+}+O^{+}$), ($C^{3+}+O^{2+}$), and ($C^{2+}+O^{3+}$) are all within 7 eV of each other. Experimentally, the ($C^{3+}+O^{2+}$) and ($C^{2+}+O^{3+}$) channels are equally probable while the ($C^{4+}+O^{+}$) channel is barely observable.

Using the data given in Tables I and II, along with the ratio of the CO^{2+} and CO^{+} production yields, which was 0.019±0.002, the relative probability for removing Q electrons in collisions of 97 MeV Ar^{14+} ions with CO molecules may be obtained. These probabilities, expressed as the ratios $Y(Q)/Y(1)$, where $Y(Q)$ is the total yield of all products resulting from the removal of Q electrons from CO, are compared with the yield ratios obtained for the ionization of Ne atoms by 97-MeV Ar^{14+} collisions in Fig. 4. It is apparent from this comparison that the ionization probabilities for CO molecules agree quite well up to $Q=4$, but become increasingly larger than those for Ne atoms beyond this point.

The solid line in Fig. 4 shows the relative ionization cross sections for Ne given by an independent-electron-approximation calculation, similar to that described in Ref. [12], in which the impact-parameter-dependent single-electron ionization probability was represented by the simple exponential function $p_0\exp(-b/r_L)$. The value of the parameter p_0 that gave the best fit to the data was 0.7. The relative ionization cross sections were found to be quite insensitive to the value used for the radius parameter r_L. The present calculations for Ne were performed using the most-probable L-electron radius, 0.335 Å, for this parameter. Corresponding cross sections for CO were calculated using the same p_0 value as for Ne, a radius parameter value of 1.13 Å, and ten as the number of valence electrons (instead of eight as for Ne). These results are shown by the dashed line in Fig. 4 and they indicate that the cross-section enhancements cannot be entirely attributed to the fact that CO has more valence electrons than Ne and is a somewhat larger target.

Part of the enhancement of the ionization probability for CO might be due to K-shell vacancy production followed by Auger decay. Similar charge multiplication effects caused by Auger decay of L vacancies have been observed in collisons of 1-MeV/amu O and F ions with Ar [12]. The dominant mechanism for K-vacancy production in the $Ar^{14+}+CO$ collision system is electron capture to the Ar L shell [13]. However, this same mechanism must also contribute to the Ne results. In fact, the electron-capture cross sections are expected to be larger for Ne than for CO since the K-binding energy of Ne more closely matches the L-binding energy of Ar.

From the above discussion, it must be concluded that much of the ionization probability enhancement is caused by a mechanism that is unique to CO. One such possibility is linked to the electron exchange that must occur between the ion with the lowest charge and its more highly charged partner during the early stages of the dissociation process in order to symmetrize the charge division. According to the classical overbarrier model of charge exchange [14], the exchange of electrons is expected to proceed from the L shell of the lower charged ion to the M shell of the higher charged ion. Thus, one of the dissociation products might be left in an excited state that would subsequently decay by an LMM Auger transition, thereby increasing its charge. One problem with this hypothesis is that the excited state would have to contain at least two M-shell electrons in order to undergo LMM Auger decay. However, such configurations could arise as a consequence of the transfer of two or more electrons in the rearrangement process, or as a result of electron excitation during the collision followed by one-electron transfer. The yield data for $Q=4$ and 5 in Table II provide some support for this scenario. The arguments based on minimum excitation energies presented above lead one to expect equal yields of ($C^{2+}+O^{2+}$) and ($C^{3+}+O^{+}$) ion pairs, while expermentally the yield of

the former is a factor of 3.4 larger than the yield of the latter. However, only the asymmetric charge division pairs will have a tendency to undergo charge exchange, which means that most of the $(C^{3+}+O^{+})$ and $(C^{+}+O^{3+})$ pairs produced in the collision will end up as $(C^{3+}+O^{2+})$ and $(C^{2+}+O^{3+})$ pairs as a result of electron transfer followed by *LMM* Auger decay. The net effect of this will be to reduce the yields of the asymmetric $Q=4$ ion pairs and increase the yields of the $Q=5$ ion pairs.

V. CONCLUSIONS

The dissociation fractions for CO^{+} and CO^{2+} molecular ions, and the branching ratios for the most prominent charge division channels of CO^{Q+} with $Q=2-7$, were determined from TOF singles and coincidence data. The characteristics of the dissociation fractions and yield ratios for CO^{+} and CO^{2+} produced in 97-MeV Ar^{14+} collisions were found to be similar to those observed for low-energy H^{+} and He^{2+} projectiles in the same perturbative regime relative to the CO valence electrons. The dissociation fraction for CO^{+} produced by valence-electron photoioniztaion at 280 eV, on the other hand, is much larger than those observed for ion-impact ionization. An analysis of the ion-pair production yields revealed a preference for symmetric or near-symmetric charge division channels, more or less in accordance with expectations based on the minimum excitation energies required for their production. The observation of an enhancement in the ionization probabilities of CO for high Q over those obtained for Ne suggested that electron transfer during the early stages of the dissociation process followed by *LMM* Auger decay plays an important role in determining the final charges of the dissociation products.

ACKNOWLEDGMENTS

This work was supported by the Division of Chemical Sciences of the U.S. Department of Energy and the Robert A. Welch Foundation.

*Present address: Institut Curie, 11 rue Pierre et Marie Curie, 75231 Paris CEDEX 05, France.

†Present address: GSI, Plasmafisikgroup, D-6100 Darmstadt, Germany.

‡Present address: Weizmann Institut, Rehovot 76100, Israel.

§On leave from the Department of Physics, Faculty of Science and Mathematics, University of Zagreb, Croatia.

[1] G. Sampoll, R. L. Watson, O. Heber, V. Horvat, K. Wohrer, and M. Chabot, Phys. Rev. A **45**, 2903 (1992).

[2] A. P. Hitchcock, P. Lablanquie, P. Morin, E. Lizon, A. Lugrin, M. Simon, P. Thiry, and I. Nenner, Phys. Rev. A **37**, 2448 (1988).

[3] M. B. Shah and H. B. Gilbody, J. Phys. B **23**, 1491 (1990).

[4] A. S. Newton and A. F. Sciamanna, J. Chem. Phys. **53**, 132 (1970).

[5] Channelplate Charged Particle Detectors (unpublished report by Comstock Incorporated, P.O. Box 199, Oak Ridge, TN 37830).

[6] V. Chamelton, Acta Electronica **14**, 225 (1971).

[7] J. L. Wisa, Nucl. Instrum. Methods **162**, 587 (1979).

[8] D. J. Ruggieri, IEEE Trans. Nucl. Sci. **NS-19**, 74 (1972).

[9] K. Tobita, H. Takeuchi, H. Kimura, Y. Kusama, and M. Nemoto, Jpn. J. Appl. Phys. **26**, 509 (1987).

[10] R. Olsen, J. Phys. B **12**, 1843 (1979).

[11] E. Merzbacher, in *Fundamental Processes in Energetic Atomic Collisions,* Vol. 103 *of NATO Advanced Study Institute, Series B: Physics,* edited by H. O. Lutz, J. S. Briggs, and H. Kleinpoppen (Plenum, New York, 1983), p. 319.

[12] O. Heber, G. Sampoll, B. B. Bandong, R. J. Maurer, R. L. Watson, I. Ben-Itzhak, J. L. Shinpaugh, J. M. Sanders, L. Hefner, and P. Richard, Phys. Rev. A **39**, 4898 (1989).

[13] S. Andriamonje, J. F. Chemin, J. Roturier, B. Saboya, J. N. Scheurer, R. Gayet, A. Salin, H. Laurent, P. Auger, and J. P. Thibaud, Z. Phys. A **317**, 251 (1984).

[14] H. Ryufuku, K. Sasaki, and T. Watanabe, Phys. Rev. A **21**, 745 (1980).